

Stress-strain analysis of SLC mine design in Kyrgyzstan

N. Bar & A. McQuillan

*Gecko Geotechnics, Kingstown, Saint Vincent and the Grenadines
neil@geckogeotech.com (email of corresponding author)*

D. Smagulov, M. Tashtanov, O. Vilchik, N. Teleu & F. Zhumadylov

KAZ Minerals, Bishkek, Kyrgyzstan

Abstract

Bozymchak is an open-pit copper mine in Kyrgyzstan that is currently transitioning from open pit to underground mining using sub-level caving method (SLC). Longitudinal SLC mining is planned to continue downward from the base of the existing open pit until mine closure.

Several geotechnical investigations were completed to understand ground conditions in the deeper areas of the deposit. These included diamond core drilling, mapping of capital developments and the modelling of major geological structures.

Three-dimensional (3D) stress-strain analysis was completed using the finite element method (FEM) to identify areas of risk forming from high stresses in response to SLC extraction. This paper briefly describes the stress-strain modelling, risks identified with the SLC sequence, and planned control measures to mitigate those risks.

Keywords

Finite element method, stress-strain analysis, underground mining, sub-level caving.

1 Introduction

Bozymchak copper-gold mine is located in the Alu-Buka district of the Jalal-Abad region of Kyrgyzstan, approximately 600 km south-west of Bishkek, the capital of Kyrgyzstan; and 150 km to the east of Tashkent, Uzbekistan, Figure 1.

Bozymchak mine has an average copper content of 1.12 %, gold grade of 1.96 g/t and silver grade of 13.2 g/t (Nikonorov, 2009; Pak et al. 2022).

The mine is currently transitioning from open pit to underground mining. The reserves are planned to be extracted within a limited time by sub-level caving (SLC) method. Due to the challenging geotechnical conditions, it was identified that caving posed a significant risk to the stability of the existing, depleted open pit (Avdeev et al. 2021). As a practical control measure to reduce the impact of this risk, pit backfilling commenced in 2023, Figure 2.

This paper discusses the stress-strain modelling to understand risks that may develop in response to the SLC sequence, and the planned control measures to mitigate those risks.



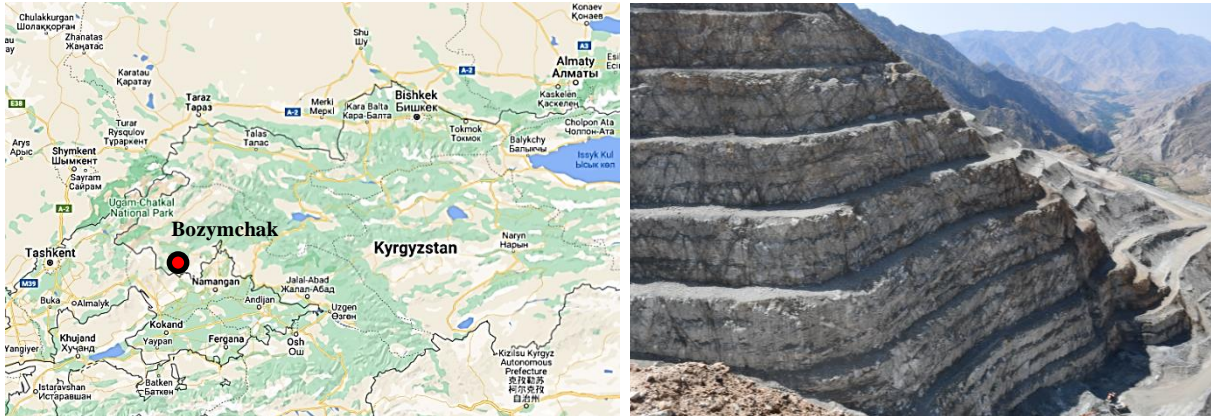


Fig. 1 Left: Bozymchak Copper-Gold Mine Location. Right: Bozymchak Open Pit nearing completion in 2022, looking south at granodiorite hanging wall (inter-ramp angle, IRA = 63°).

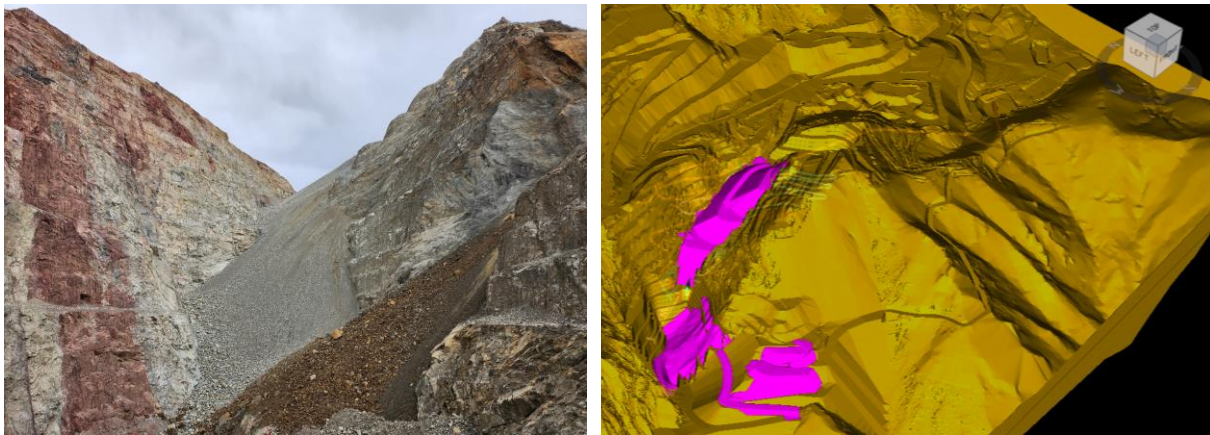


Fig. 2 Left: Bozymchak pit backfilling in November 2023 looking east (limestone footwall on left). Right: Backfill design shown in pink.

2 Mining Context

From 2012 to 2023 the Bozymchak deposit has been partly extracted through open pit mining at a rate of 1.1M tonnes of ore per year to a depth of 300 m. Ore has been processed on site using a plant with 1.1M tonne capacity per annum. Underground mine development in preparation for SLC mining commenced in 2018 and was completed in September 2023.

Longitudinal SLC mining with an initial capacity of 300,000 tonnes of ore per year began at elevations 2130 m and 2105 m. Based on the life-of-mine plan, SLC mining is expected to reach a production rate of 1.1M tonnes of ore per year from 2024. The life of the underground mine is nine years with proven and probable ore reserves of 9.6M tonnes with a content of 0.73% copper, 1.14 g/t gold and 7.29 g/t silver.

Backfilling of the pit using waste rock fill, as shown in Figure 2, will progressively fill the extracted portions of the SLC with gravity. SLC mining will utilize various types of diamond-shaped ring cross-sections depending on the sub-level drift spacing which will range from 15 to 28 m, Figure 3. The standard spacing of the sublevel drifts is 25 m with a 65° shoulder angle on the rings.

Predicted average dilution during production is 21% with an ore loss of 8%. The predicted dilution is similar to most SLC mines around the world, which range from 4 to 43% (Campbell, 2022). However, the predicted ore loss is considerably less than most SLC mines, which are typically 10 to 20%.

Currently, the mine is investigating options for switching from diamond-shaped rings to fan-shaped rings in order to reduce the required blast hole lengths and drift spacing for improving ore extraction.

Rings are drilled using 102 mm diameter holes with lengths of 10 to 50 m with a Sandvik DL421 top hammer long-hole drill rig. ANFO granular explosives are used for blasting.

Face drilling and supporting of mine development and drifts are carried out using Sandvik DD321 two-boom jumbos. Mucking and haulage is carried out using Sandvik LH410 loaders and TH430 dump trucks.

The mine requires approximately 3.6 to 4.0 m³/s of fresh air per 1,000 tonnes of ore production per month, which is similar to other SLC mines. Groundwater inflows in the lower levels of the mine are expected to range from 25 to 90 m³ per hour depending on the season.

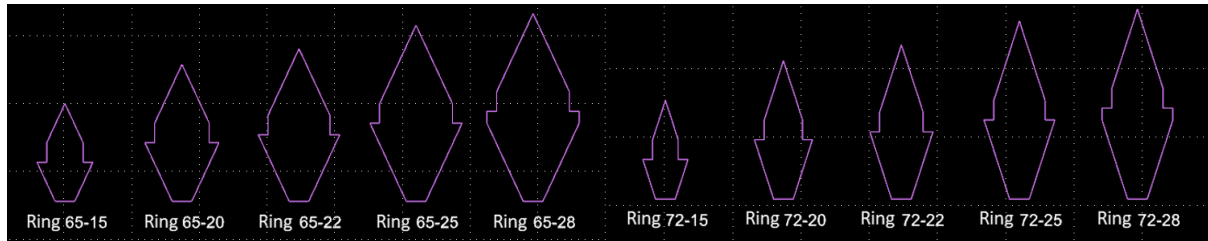


Fig. 3 Design Ring Cross-Sections for SLC Mining.

3 Geological Setting

The Bozymchak copper-gold (Cu-Au) skarn deposit is located within in the Chatkal-Kurama region of the Tian Shan belt (Abzalov et al. 2019; Zu et al. 2019). The 305 Ma skarn deposit is associated with a granodiorite porphyry intrusion, Figure 4.

Sedimentary, intrusive, and metamorphic rocks form the key stratigraphic units within the Bozymchak Cu-Au deposit. Rock types comprise marbled and dolomitic limestones, skarn, serpentinite and granodiorite (from top-down; Alpiev et al. 2023):

- Limestones form the hanging wall and are very strong, coarsely bedded with minor fracturing.
- Skarns of ore bodies are timed to coincide with the contact of the granodiorite intrusion with limestone.
- Serpentinites are the weakest rocks in the deposit and alternate with skarn blocks. Serpentinite is prone to unravelling, particularly when in contact with water.
- Granodiorites form the hanging wall and are strong with discontinuous jointing.

Figure 5 displays a plan and cross-section of the Bozymchak deposit and planned SLC.

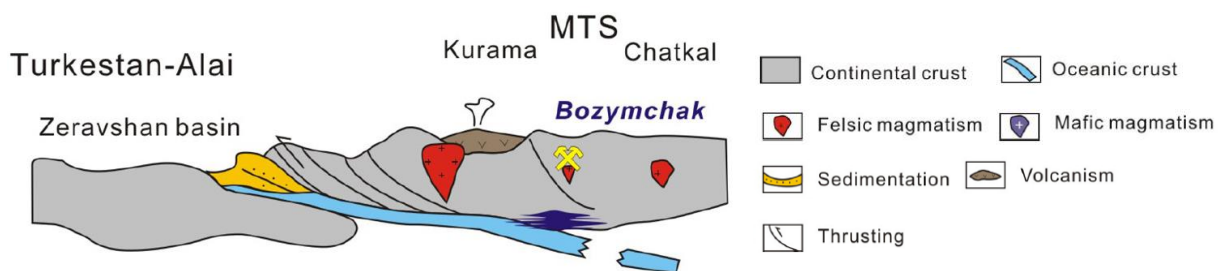


Fig. 4 Tectonic settings and evolution of Chaktal-Kurama Middle Tian Shan (MTS) mountain ranges and related Cu-Au mineralization at Bozymchak (Zu et al. 2019).

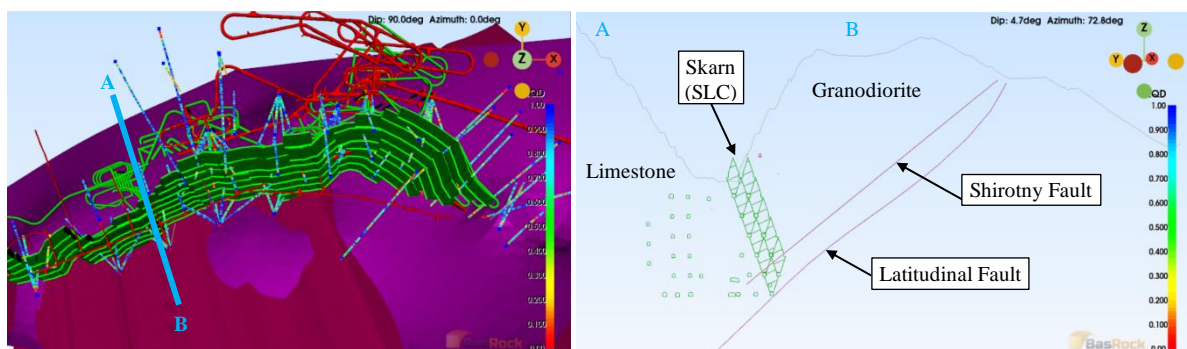


Fig. 5 Left: SLC plan showing drilling data (RQD) relative to Latitudinal and Shirotny Faults. Right: Cross-section A-B of SLC plan looking east.

The Latitudinal Faults are related to the distribution of the sulphide mineralization at the deposit and have resulted in the downward displacement of part of the orebody by 200 to 280 m (Alparov, 2020). A complex series of steeper geological faults are present at deposit, crosscutting the Latitudinal Faults and separating the orebody into various blocks.

4 Geotechnical Investigation

Several geotechnical investigations have been completed at Bozymchak to understand strength and stiffness properties of the different rock masses. Table 1 presents initial intact rock properties for the hanging wall and footwall (Alpiev et al. 2023).

Table 1 Intact Rock Properties (Alpiev et al. 2023)

Rock Type	Unit Weight (kN/m ³)	UCS, σ_c (MPa)	UTS, σ_t (MPa)	Young's Modulus, E_i (GPa)	Poisson's Ratio, ν	V_p (km/s)	V_s (km/s)
Limestone (Footwall)	27	45 - 87	4 - 7	63	0.18	5.9	2.7
Granodiorite (Hanging Wall)	29	171	14	56	0.18	5.5	2.5

Site investigations also included several diamond drilling campaigns to improve geological and geotechnical understanding. These included assessments of rock mass quality, RQD (Deere, 1963), RMR₈₉ (Bieniawski, 1989); and the Q-system (Barton et al. 1974; Grimstad & Barton, 1993). Face mapping has been used to validate and update the geotechnical model with the progression of capital developments as shown in Figure 6.

Based on the Q-system and considering static, in-situ stresses (i.e. without considering mining-induced stresses), rock mass quality in the footwall and hanging wall is typically *Fair to Good* (Q values ranging from 4 to 20), for Limestone, Figure 6. In close proximity to the contact with the skarn orebody and near geological faults, rock mass quality can be *Very Poor to Poor* ($Q \approx 1.0$).

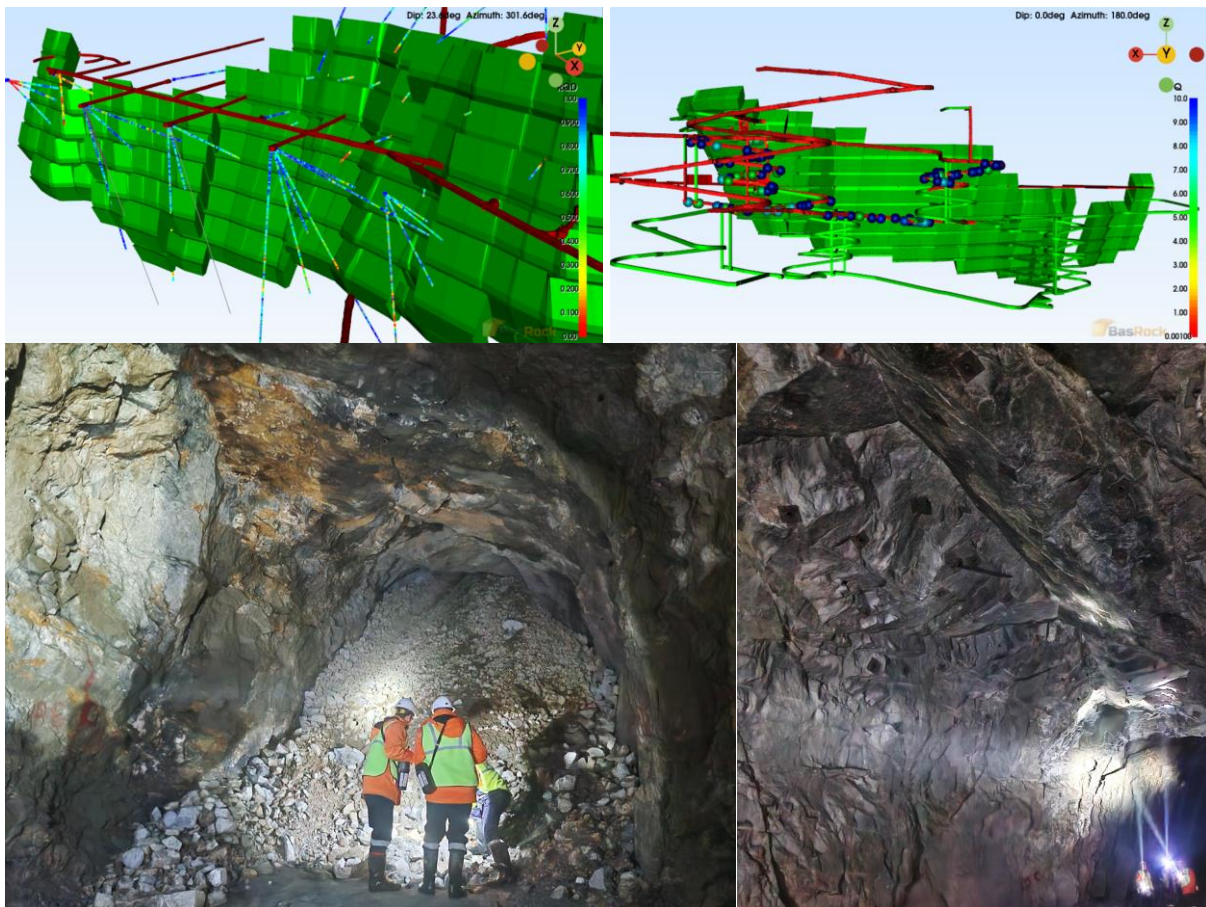


Fig. 6 Top: Geotechnical site investigations including diamond drilling into planned SLC hanging wall (top-left: showing RQD) and face mapping of capital developments (top-right: showing Q). Note: red denotes constructed development drifts; green denotes planned developments and SLC. Bottom: Examples of typical rock mass quality for limestone. Bottom-Left: $Q \approx 4$ with some overbreak near a SLC drawpoint. Bottom-Right: $Q \approx 10$ with overbreak in capital development.

5 Geotechnical Model

The geotechnical model was developed based on the lithological (rock type) model and the available intact rock and rock mass quality data which is summarized in Table 2. Based on face mapping data including intact rock strength estimation in the field and geological strength index (GSI) assessments, the rock mass strength properties were derived using the Hoek-Brown failure criterion (Hoek & Brown, 2019). Rock mass stiffness parameters, including Young's Modulus, was estimated using the approach by Hoek & Diederichs (2006).

Table 2 Rock Mass Strength and Stiffness

Rock Type	RQD (%)	J_n	Q^*	UCS (MPa)	GSI	m_i	Young's Modulus, E_m (GPa)	Poisson's Ratio, ν
Limestone	75	3	4.000	75	71	12	11	0.3
Granodiorite	70	6	10.000	150	64	29	12	0.3
Skarn	70	6	1.000	125	60	29	10	0.3
Serpentinite	40	12	0.200	100	25	15	1	0.3

* Considering in-situ stress state only

Regional fault zones were characterized using the Mohr-Coulomb failure criterion based on rudimentary wedge failure back-analysis from the open pit (140 m high failure) and engineering judgement: $c' = 100$ kPa; $\varphi' = 25^\circ$; $E_m = 0.5$ GPa; $\nu = 0.3$.

No in-situ stress measurements were completed at the site; however, it was understood that anisotropic in-situ stresses were present with the horizontal to vertical stress ratio, σ_h / σ_v , ranging from 1.5 to 2.

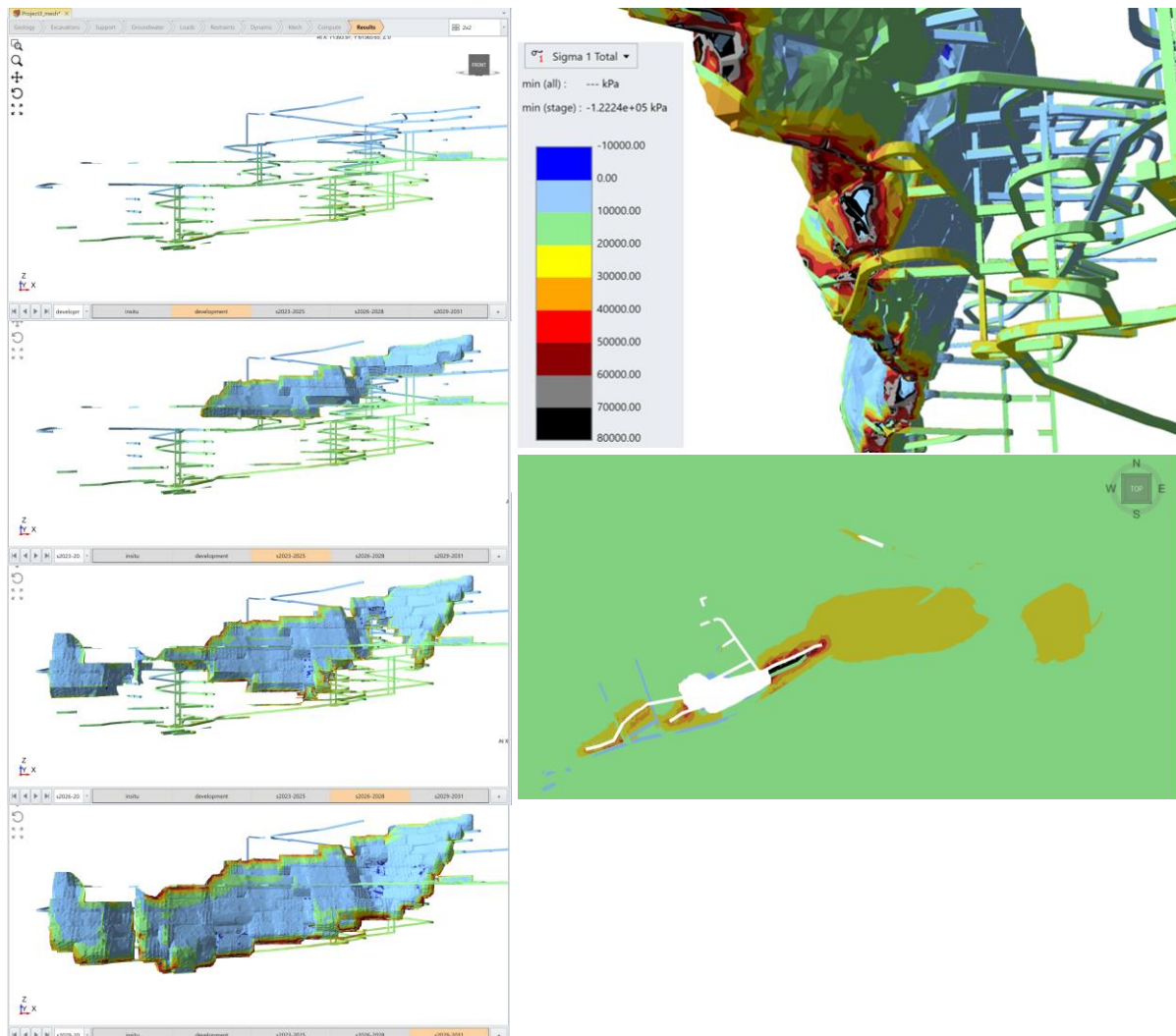


Fig. 7 3D FEM results showing Maximum Principal Stress (σ_1) acting on the underground excavations (pit not shown for clarity). Left (top to bottom): Stages 2, 3 4 & 5. Right: Maximum Principal Stress (σ_1) locally exceeding 80 MPa on 1930L in near Shirotny Fault.

6 Stress-Strain Model

A three-dimensional (3D) stress-strain model was developed using finite element method (FEM) RS3 software by Rocscience, Inc. The model comprised the latest topographical surveys including the final pit design, 2022 lithology (geology) and major structure (fault) models and the proposed underground development and SLC design. Model stages were used to sequence excavations, Figure 7. The excavation sequence was simplified as follows to reduce model computational time:

1. Stage 1: In-situ conditions at end of 2022 including all existing underground developments surface excavations (including end of pit design).
2. Stage 2: Excavation of all underground capital and mine production development.
3. Stages 3 to 5: SLC Excavation between 2023 and 2031.

The stress-strain model uses a four-noded, graded tetrahedra mesh comprising almost 18 million elements with a minimum size of 3 m applied to the underground excavations.

Model assumptions included dry conditions given the topographic elevation of most of the deposit. Materials were considered to be elastic, meaning they cannot ‘fail’ in the model, but can be assessed using a failure envelope or Strength Factor. Initial element loading for the models including body force due to gravity and field stresses: $\sigma_h / \sigma_v = 2$.

As shown in Figure 8, the Strength Factor on the hanging wall is less than one (i.e. shear failure) between Stages 3 to 5. That is, the hanging wall is not expected to remain stable and should experience overbreak to a depth of approximately 50 m, which may be a considerable source of dilution if unmanaged. In Stage 5, the Strength Factor is less than zero for the Shirotny and Latitudinal faults, indicating tensile stresses, or fault reactivation.

Stresses increase proportionally with depth and SLC excavation progress. However, high stress concentrations are evident near the Shirotny and Latitudinal faults. As shown in Figure 7, the maximum principal stress, σ_1 , may locally exceed 80 MPa on 1930L and the maximum shear stress ratio frequently exceeds 0.4 in the pillar between the developments and the faults.

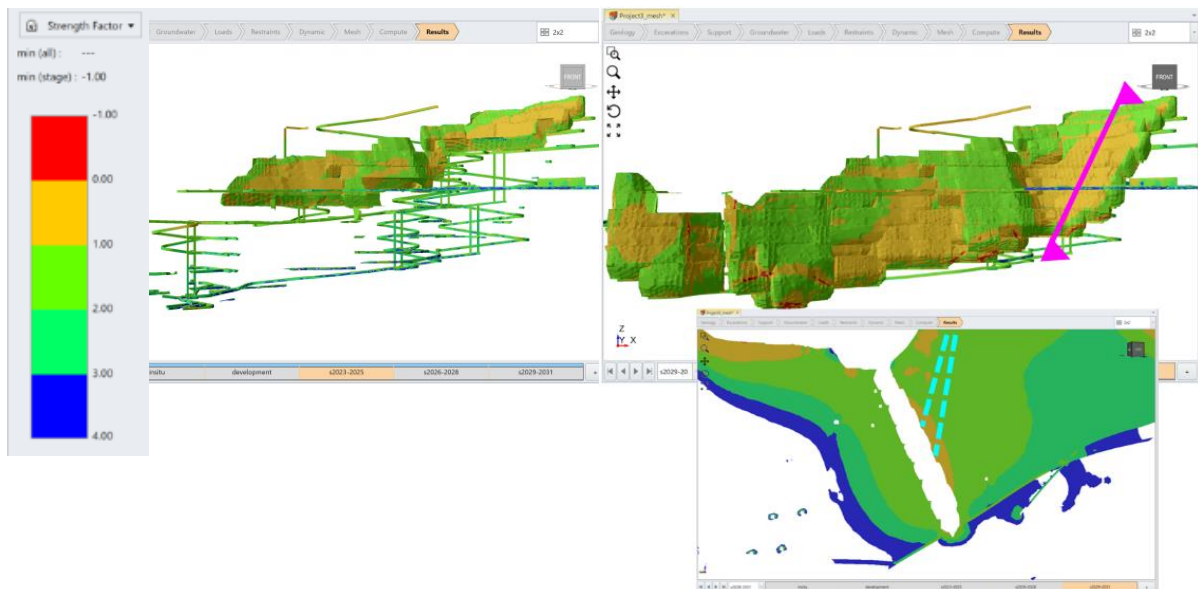


Fig. 8 3D FEM results. Left: Stage 3. Right: Stage 5. Strength Factor less than one on SLC hanging wall and less than zero in the Shirotny and Latitudinal Faults. Cross-section showing potential depth of hanging wall overbreak & proposed boreholes for monitoring.

7 Evaluation of Failure Modes and Ground Support Requirements

Numerical model outputs were used to assist in understanding potential modes of rock mass instability that the underground excavations may be exposed to at different locations and at various stages of mine development and production. Figure 9 originated from concepts and case studies by Hoek & Brown (1980) and has been developed over 40+ years to relate in-situ stress conditions using the stress

vs strength ratio and GSI (previously RMR₇₆) to indicate potential failure modes in underground excavations. At Bozymchak SLC, potential failure modes are interpreted to include:

- Block falls and wedge failures at low stresses to brittle failure of intact rock at intermediate and high stresses in Limestone, Granodiorite and Skarn.
- Unravelling to squeezing in Serpentinite from low to high stresses.

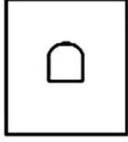
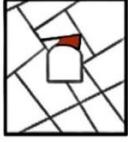
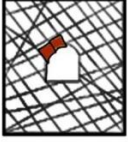
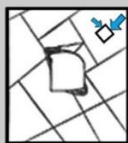
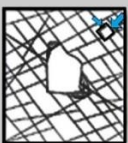
	Massive (GSI >75)	Moderately fractured (50<GSI<75)	Highly fractured (GSI<50)	
Low in situ stress ($\sigma_1/\sigma_c < 0.15$)	 Linear elastic respons.	 Falling or sliding of blocks and wedges.	 Unravelling of blocks from the excavation surface.	$D < 0.4 (\pm 0.1)$
Intermediate in situ stress ($0.4 > \sigma_1/\sigma_c > 0.15$)	 Brittle failure adjacent to excavation boundary.	 Localized brittle failure of intact rock and movement of blocks.	 Localized brittle failure of intact rock and unravelling along discontinuities.	$0.4 (\pm 0.1) < D < 1.1 (\pm 0.1)$
High in situ stress ($\sigma_1/\sigma_c > 0.4$)	 Brittle failure around the excavation.	 Brittle failure of intact rock around the excavation and movement of blocks.	 Squeezing and swelling rocks. Elastic/plastic continuum.	$D > 1.1 (\pm 0.1)$

Fig. 9 Potential failure modes based on the ratio of maximum in-situ stress and GSI (after Hoek & Brown, 1980; Martin et al. 1998; Askaripour et al. 2022)

Initial studies into ground support requirements generally only consider in-situ stresses. On 1930 L, σ_1 is approximately 20 MPa. Mining induced stresses from SLC operations will be significantly higher. Based on the stress-strain modelling, σ_1 is expected to increase to approximately 50 MPa (typical) near development drives, with maximum σ_1 values locally reaching 80 MPa. Mining induced stresses are approximately double the in-situ stress, which is considered realistic as it has occurred in other SLC mines including Kiirunavaara mine in Sweden (Jacobsson et al. 2013).

Table 3 Q values based on In-Situ and Mining Induced Stresses

Stress State	In-Situ	Mining Induced	
		Typical	Maximum
σ_1 on 1930 L (MPa)	20	50	80
Limestone	4.000	0.333	0.250
Granodiorite	10.000	0.350	0.078
Skarn	1.000	0.023	0.010
Serpentinite	0.200	0.004	0.002

Such profound changes in stresses in proximity to excavations as a result of SLC mining have an impact on the stress reduction factor, SRF_b, in the Q-system. As demonstrated in Table 3, Q values change significantly in response to mining induced stresses. That is, as SLC mining progresses, ground support requirements for different geotechnical domains will change, i.e. increase in areas subject to high mining induced stresses.

Pre-mining conditions require limited support in Limestone and Granodiorite due to relatively small spans, typically 5 m, and *Fair* rock mass quality. As shown in previous photographs, Figure 6, these excavations are generally unsupported with some spot bolting and mesh in more fractured areas (i.e. Support Category 1). However, as stresses increase in response to SLC mining, e.g. 50 MPa on 1930 L, the rock mass quality may reduce to *Very Poor* and require Support Category 4 (6-9 cm thick fibre-reinforced shotcrete and bolting). Similar increases in support will be required in the Skarns and Serpentinites; however, these are generally less prevalent, especially in long-term developments.

8 Discussion

The initial geotechnical investigations, model and stress-strain analysis provided valuable insights into expected ground behavior for the Bozymchak SLC excavations and subsidence zone. Ground support requirements in various parts of the mine are expected to significantly increase over time in response to mining induced stresses. Further assessments of ground support design are also planned and include kinematic failure modes and dynamic loading.

The stress-strain modelling has many limitations and requires validation (and future updating) with a combination of further site investigations and the routine mapping and evaluation of rock mass quality and rock mass damage.

Monitoring systems are also required to validate the overbreak in the hanging wall, subsidence zone extents, and as well as rock burst risk. Planned monitoring systems include prism monitoring and aerial photogrammetry for surface displacements and SLC material flow balances. Subsurface monitoring will include time domain reflectometry (TDR) for the hanging wall and micro-seismic monitoring. A trigger-action-response-plan (TARP) will be developed for managing subsidence and seismicity risks.

References

- Abzalov M, Djenchuraeva R, Alpiev Y, Abzalov S (2019) The geology of the Bozymchak Cu-Au skarn deposit, Tien Shan belt, Central Asia: emphasis on the geochemical characteristics of the granitoids. *Applied Earth Science* 128(3), pp. 106-123.
- Alparov A (2020) An Automated System for Monitoring Open Pit Walls taking into account Climate Properties. XII Annual International Conference on Modern Equipment and Technologies in Scientific Research, Russian Academy of Sciences in Bishkek, 22-24 April 2020, Bishkek, Kyrgyzstan, pp. 4-10.
- Alpiev Y, Shamsutdinov MM, Akmatalieva MS (2023) Geological Features and Physical and Mechanical Properties of the Bozymchak Deposit. *KRSU Bulletin* 23(4), pp. 162-168.
- Askaripour M, Saeidi A, Rouleau A, Mercier-Langevin P (2002) Rockburst in underground excavations: A review of mechanism, classification, and prediction methods. *Underground Space* 7, pp.
- Avdeev AN, Zoteev OV, Sosnovskaya EL (2021) Geomechanical situation prediction in transition from open to underground mining of steeply dipping ore body by systems with caving. *Mining Informational and Analytical Bulletin* 5(2), pp. 6-15.
- Barton N, Lien R, Lunde J (1974). Engineering Classification of Rock Masses for the Design of Tunnel Support. *Rock Mechanics* 6, pp. 189-236.
- Bieniawski ZT (1989) *Engineering Rock Mass Classifications*. Wiley, New York, 251p.
- Campbell AD (2022). A global review of recovery, dilution and draw control in sublevel caving mines. *Caving 2022*, Adelaide, Australia, 30 August – 1 September 2022, pp. 909-926.
- Deere DU (1963) Technical description of rock cores for engineering purposes. *Felsmechanik und Ingenieurgeologie* 1, pp. 16-22.
- Grimstad E, Barton N (1993). Updating of the Q-System for NMT. *Proceedings of the International Symposium on Sprayed Concrete*, 22-26 October 1993, Fagernes, pp. 46-66.
- Jacobsson L, Töyrä J, Woldemedhin B, Krekula H (2013) Rock support in the Kiirunavaara Mine. *Proceedings of Ground Support 2013*, 13-15 May 2013, Perth, Australia, pp. 401-410.
- Hoek E, Brown ET (1980) *Underground Excavations in Rock*. CRC Press, London, 536p.
- Hoek E, Brown ET (2019) The Hoek–Brown failure criterion and GSI – 2018 edition. *J. Rock Mechanics & Geotechnical Engineering* 11(3), pp. 445-463.
- Hoek E, Diederichs MS (2006) Empirical estimation of rock mass modulus. *Int. J. Rock Mechanics & Mining Sciences* 36, pp. 203-215.
- Martin CD, Kaiser PK, McCreath DR (1998) Empirical estimation of rock mass modulus. *Int. J. Rock Mechanics & Mining Sciences* 43, pp. 203-215.
- Nikonorov VV (2009) *Ore deposits of Kyrgyzstan*. Bishkek, 482p.
- Pak NT, Alpiev M, Alpiev Y (2022) Silver Mineralization at the Skarn Field Bozymchak (Kyrgyzstan). *KRSU Bulletin* 22(12), pp. 173-181.
- Zu B, Seltmann R, Xue C, Wang T, Dolgoplova A, Li C, Zhou L, Pak N, Ivleva E, Chai M, Zhao X (2019). Multiple episodes of Late Paleozoic Cu-Au mineralization in the Chatkal-Kurama terrane: New constraints from the Kuru-Tegerek and Bozymchak skarn deposits, Kyrgyzstan. *Ore Geology Reviews* 111: 103077.